

Kinetics, equilibrium and thermodynamics studies of Direct Red 1 dye adsorption on groundnut shell based activated carbon

Umar Isah Abubakar ^{1*}, AbdurRaheem Giwa ², AbdusSalam Ibrahim ¹,
 Salisu Muhammad ¹, and Mustafa Abdullahi ¹

¹Product and Process Development (PPD) Research Group, Department of Chemical Engineering, Ahmadu Bello University, Zaria, 810271, Nigeria.

²Department of Polymer and Textile Engineering, Ahmadu Bello University, Zaria, Nigeria.

Received 12 June 2022,
 Revised 17 Sept 2022,
 Accepted 18 Sept 2022.

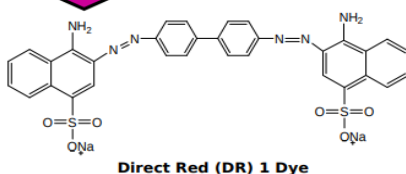
Keywords

- ✓ Groundnut Shell Activated Carbon,
- ✓ Direct Red 1 Dye,
- ✓ Adsorption,
- ✓ Kinetics,
- ✓ Equilibrium,
- ✓ Thermodynamics.

iaumar@abu.edu.ng,
isahaumar6@gmail.com,
 Phone: +2348033581563

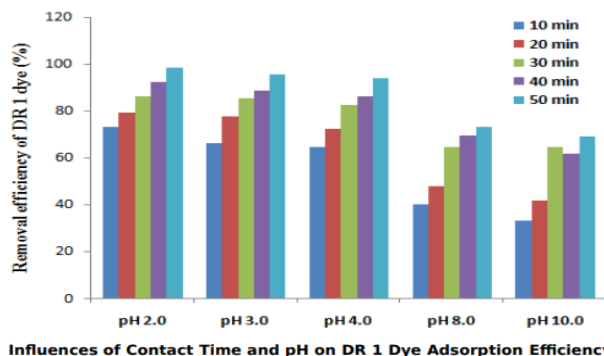
Abstract

In this study, activated carbon derived from groundnut shells (GSAC) was produced from the by-product of agricultural products for the kinetics, equilibrium, and thermodynamics studies of Direct Red 1 (DR 1) dye adsorption from aqueous solution. GSAC was characterized using the field emission dual beam-scanning electron microscopy/focused ion beam (FES-SEM/FIB), Fourier transforms infrared spectroscopy (FT-IR), and UV/visible spectrophotometer. Adsorption experiments were carried out using batch mode in order to investigate the effects of contact time (10–50 min), temperatures (28°C–50°C), initial dye concentration (10–50 mg/L), and pH (2–10) on the removal of DR 1 dye. Pseudo-first-order and pseudo-second-order kinetics' models were employed for the fitting of observed kinetic data. The experimental data was found to be best described by pseudo 2nd order kinetic model. It was noted that the observed specific adsorption rate constant (k_{obs}) for its kinetics increased by 61.96% and 59.70% when the temperature was increased from 301 K to 313 K, and from 301 K to 323 K, respectively. The activation energy (E_a) was determined as 6.35 kJ/mol. Langmuir and Freundlich isotherm models were utilized for the fitting of equilibrium data with good correlation coefficients (i.e., Pearson's r) and coefficients of determination (i.e. adjusted R^2). Thermodynamic analysis reveals that the adsorption process was spontaneous, the changes in entropy (ΔS) and enthalpy (ΔH) were found to be 0.07 kJ/mol K and 18.31 kJ/mol, respectively. GSAC was shown to be a promising adsorbent for the adsorption of DR 1 dye from aqueous solutions.



Summary for the Pseudo-second-order DR 1 Dye Adsorption Kinetics

Temp. (K)	Pseudo-second-order kinetic model				
	q_e , cal (mg g ⁻¹)	k_{obs} (g mg ⁻¹ min ⁻¹)	T_{AO} (mg L ⁻¹ min ⁻¹)	Pearson's r	Adj. R^2
301	3.115	2.61×10^{-2}	2.54×10^{-1}	0.993	0.979
313	5.261	2.42×10^{-2}	6.69×10^{-1}	0.998	0.995
323	5.456	2.19×10^{-2}	6.52×10^{-1}	0.995	0.986



1. Introduction

Presently, more than 10,000 dyes commercially exist with a global yearly production in surplus of 7×10^5 million tons and approximately 5–10% of these dye-stuffs are ejected into water as wastes [1]. Of all these class of dyes, Azo dyes are the largest class of synthetic dyes since it accounts for 60–70% of the dye's total utilization in dyeing and printing applications [2]. Its prolonged uses show that most of the Azo dyes and their reaction products have carcinogenic consequences, which indicates that it is very necessary to eliminate the dyes from the industrial wastewater previous to the wastewater disposal. However, the wastewater containing Azo dyes are very difficult to decolorize because they contain one or more Azo groups with aromatic ring and sulfonate groups in their chemical structure which induce that they are resistant and stable at aerobic digestion and oxidizing agent environment, respectively.

Globally, synthetic dyes are extensively used in textile, paper, printing, plastic, leather and cosmetic industries. An assortment of pollutants such as dyes, degradable organics, surfactants, heavy metals, pH adjusting chemicals, etc., can be established in textile wastewater [3]. In addition, colored effluent can have an effect on photosynthetic processes of aquatic plants, plummeting oxygen levels in water and in stern cases, resulting in the suffocation of aquatic flora and fauna [4,5]. Among the synthetic dyes is C. I. Direct Red 1 (DR1), commercially called Congo red (CR) and also known as (disodium 4-amino-3-[[4-[4-[(1-amino-4-sulfonatophthalen-2-yl)diazenyl]phenyl]phenyl]diazenyl]-naphthalene-1-sulfonate), which has two azo bonds (-N=N-) chromophores in its molecular structure. This is a typical example of anionic diazo dyes that can be obtained by coupling tetrazotised benzidine with two naphthionic acid molecules. It is also the earliest synthetic dye produced, which can directly dye cotton materials. DR1 is a linear anionic secondary diazo dye, it is soluble in many organic solvents, but yielding red colloidal fluorescent solutions in aqueous media due to its hydrophobicity made by the presence of biphenyl and naphthalene groups in the molecule [6]. The postulated mechanism for DR1 aggregation is by hydrophobic interaction involving the π - π bonds of the aromatic rings making planar structures [7].

Since DR1 dye was often used in the dyeing process in many industries, it was used as a representation of synthetic dye in this study. Owing to its structural stability and complex structure, wastewater containing DR1 are resistant to biodegradation [8,9,10]. Moreover, DR1 has also been known as a highly toxic substance, unpleasant and suspected to be mutagenic and carcinogenic. These negative features will lead to a variety of hazards that pose a significant risk to the environment and human health. Therefore, the treatment of DR1 dye effluent is very important. However, the traditional physical, chemical and biological means of wastewater treatment often have little degradation effect on this anionic secondary diazo dye pollutant due to their complex aromatic structures, which provide them with physicochemical, thermal and optical stability [11]. DR1 was frequently used in the dyeing process for many industries such as textiles, leather, food, paper, printing, pharmaceutical, cosmetics, etc. However, the waste water produced from these industries involving DR1 has contributed to serious environmental issues due to its natural aesthetic, where the colours can be seen even at low concentrations [9]. The reactive azo DR1 dye, which is also difficult to biodegrade, was not affected by the conventional treatment. Therefore, pollution caused by industries involving DR1 may become a huge problem in the future without proper pollution control.

Adsorption is one of the most practicable and widely used powerful techniques for getting rid of different sorts of contaminants [12]. It has been successfully employed in the treatments of various dyes from textile wastewater by decolorization of the effluents [13]. However, one of the major demerits of the adsorption is the high costs of purchasing the commercial grade activated carbon for the textile

wastewater treatments. As a result, this obliges the need for the low cost adsorbents. Consequently, there is a growing interest in the development and application of activated carbon derived from agricultural by-products. One of the potential abundant by products that can be transformed into low cost activated carbon and applied for wastewater treatment as well as water purification is the groundnut shells. The total production of the groundnut reported in 2007 was 34.9 million metric tons [13]. However, very little attention is paid to utilization of groundnut shell agricultural waste for the development of low-cost adsorbents for potable water purification and wastewater treatment.

The profitable operation of adsorption processes solely rely upon the properly designed adsorber. An efficient adsorber can only be designed and developed after fully understanding the kinetics, equilibrium and thermodynamic parameters. Specific rate constant and order of the adsorption are the relevant kinetic parameters that play an essential role in characterizing the rate of adsorption and the adsorber design. These pertinent data are required in the development of any kind of functional adsorber at different sizes such as bench, pilot, and commercial scales. Many studies have been reported on the kinetics, equilibrium and thermodynamics of different sorts of dyes adsorption on activated carbon and other material derived from agricultural by products [14-24]. However, there is no such report on DR 1 dye adsorption onto groundnut shell based activated carbon in the open literature to the best of our knowledge. The current studies involve the kinetics, equilibrium and thermodynamics studies of DR 1 dye adsorption onto activated carbon derived from groundnut shells.

2. Methodology

2.1 Production and characterization of groundnut shell activated carbon

Groundnut shell was obtained from Zaria. The production processes consist of drying and particle size reduction of the groundnut shells, activation of the ground samples with 100 cm³ solution of 45% or 50% (w/v) phosphoric acid concentration for 12 hours impregnation time, followed by carbonization in a furnace at a temperature between 400 and 600°C for 1 hour.

2.2 Adsorbate

Distilled water was used for washing and filtering the end product several times until the pH falls between 6.44 and 6.87. Then, it was completely dried in an oven at 110°C for 6 hours. Direct Red 1 (DR 1) dye was obtained from the Department of Textile Science (now Polymer and Textile Engineering Department), Ahmadu Bello University, Zaria. It was chosen from the class of azo dyes and employed as the model adsorbate in the present investigations due to their wide application. DR 1 has a beautiful molecular structure as shown in Figure 1 with the main functional group as vinyl sulphone.

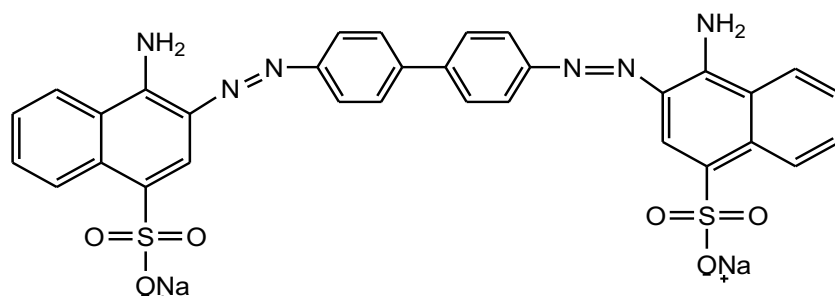


Figure 1. Molecular structure of Direct Red 1 dye

It has a commercial name popularly known as *Congo Red*. The colour index (C.I.) number of DR 1 is 22310, CAS number of 2429-84-7, molecular weight of 696.68 gmol⁻¹, molecular formula of C₃₂H₂₂N₆O₆S₂Na₂, Lambda max of 500 nm, and solubility of 30 g/L in water at 80 °C. A stock solution

of 200 mg/L of DR 1 in distilled water was prepared. The pH was determined to be 6.23. Desired concentrations of the working solutions were prepared by successive dilution of the stock solution.

2.3 Adsorption kinetics and equilibrium studies

The adsorption experiments for the kinetics and equilibrium studies were conducted batch wise in a 250 mL conical flask. 100 mL of 50 mg/L of the standard working solutions of the DR 1 dye solution was mixed with 1.0 g of the GSAC adsorbent. Then, the mixture was stirred thoroughly at the following temperatures: 28°C ambient condition, 40°C, and 50°C with constant speed of 350 rpm of a magnetic stirrer for pH from (2–10), initial dye concentration from (10–50 mg/L), and contact time from (10–50 min) in a hot plate. After attaining the equilibrium, a vacuum pump filter was used for filtering the mixture. The absorbance of each sample at the maximum adsorption wavelength ($\lambda_{\max}=500\text{nm}$) of the DR 1 dye solutions were observed, measured, and recorded using UV/Visible spectrophotometer at the beginning and at the end of each experiment. The quantity of adsorbate adsorbed at equilibrium, q_e (mg/g) was determined using Eqn. 1. The two experiments for the adsorption kinetics and equilibrium studies were similar. However, the only difference was that the experiments for the kinetics studies were observed at specified time intervals. The quantity of adsorbate, q_t (mg/g) at time t , and the removal efficiency of DR 1 dye, R (%) were estimated using Eqns. 2 and 3, respectively.

$$q_e = \frac{C_0 - C_e}{M} \times V \dots \dots \dots (1)$$

$$q_t = \frac{C_0 - C_t}{M} \times V \dots \dots \dots (2)$$

$$\text{Removal efficiency, } R(\%) = \frac{C_0 - C_t}{C_0} \times 100 \dots \dots \dots (3)$$

Where M is the mass of the adsorbent used (g), C_0, C_e, C_t (mg/L) are the liquid phase concentrations of adsorbate (DR 1 dye) at initial, equilibrium, at any time t (min), respectively, R is the DR 1 dye removal efficiency in (%) and V is the volume of the solution (mL).

2.3.1 Adsorption kinetics

In describing the kinetics of DR 1 dye adsorption onto the GSAC, the kinetic models for pseudo-first-order, pseudo-second-order and intra-particle diffusion were utilized.

The model for the pseudo first-order kinetic expression

The rate law for the pseudo first-order adsorption of the DR 1 dye onto GSAC can be expressed according to Lagergren, [25] as shown in Eqn. 4.

$$\frac{dq_t}{dt} = k_1(q_e - q_t) \dots \dots \dots (4)$$

where k_1 (min⁻¹) is the observed specific rate constant for the pseudo first-order adsorption kinetic model. Using the boundary conditions: $q_t = 0$ at $t = 0$ and $q_t = q_t$ at $t = t$ for integrating Eqn. 4, and rearranging into a linear form gives Eqn. 5:

$$\log(q_e - q_t) = \log q_e - \frac{k_1}{2.303} t \dots \dots \dots (5)$$

It is observed that q_e and k_1 can be found from the intercept and slope of the plots of $\log(q_e - q_t)$ versus t for different kinetic data at different conditions as shown in Eqn. 5.

The model for the pseudo second-order kinetic expression

Similarly, the rate law for the pseudo second-order adsorption of DR 1 dye onto the GSAC can be expressed based on the relation reported by Ho and McKay [26] as shown in Eqn. 6.

$$\frac{dq_t}{dt} = k_2(q_e - q_t)^2 \dots \dots \dots (6)$$

Where k_2 (min g mg⁻¹) is the observed specific rate constant for the pseudo second-order adsorption kinetic model. Using the boundary conditions: $q_t = 0$ at $t = 0$ and $q_t = q_t$ at $t = t$ for integrating Eqn. 6, and rearranging into a linear form produces Eqn. 7.

$$\frac{t}{q_t} = \frac{1}{k_2 q_e^2} + \frac{t}{q_e} \dots \dots \dots (7)$$

The initial adsorption rate can be considered from Eqn. 7 when t approaches 0, to be as shown in Eqn.8:

$$r_{A0} = k_2 q_e^2 \dots \dots \dots (8)$$

Hence, the initial adsorption rate for DR 1 dye, r_{A0} (mg L⁻¹min⁻¹), q_e and q_e can be determined experimentally from the slope and intercept of the plots of t/q_t versus t for different kinetic data at different conditions as shown in Eqns. 7 and 8.

The model for the intra-particle diffusion expression

The likelihood for intra-particle diffusion step to control the adsorption rate of DR 1 dye onto the GSAC was examined using the expression reported by Weber and Morris [27] as shown in Eqn. 9.

$$q_t = k_{id} t^{1/2} + C_i \dots \dots \dots (9)$$

Where C_i is the resistance to the mass transfer across the film, and k_{id} is the adsorption rate constant for intra-particle diffusion. If intra-particle diffusion controls the process (i.e. the rate-limiting step), then plots of q_t versus the square root of time ($t^{1/2}$) would give a straight line. The values of k_{id} and C_i can be found from the slope and intercept of the Eqn. 9 plots.

The temperature effects on the adsorption

The influence of temperature on the adsorption of the DR 1 dye onto the GSAC was examined by varying the temperature regimes of the adsorption which in turn affects the activation energy of the process and perhaps have dominant effects on the specific adsorption rate constant. The expression reported by Arrhenius [28] as shown in Eqn. 10 was used in estimating the activation energy of the adsorption.

$$k(T) = A e^{\frac{-E}{RT}} \dots \dots \dots (10)$$

Taking the logarithms both sides of Eqn. (10) give Eq. (11).

$$\ln k(T) = \ln A - \frac{E_a}{R} \left(\frac{1}{T} \right) \dots \dots \dots (11)$$

where k is the specific rate constant of adsorption, A is the frequency factor or pre-exponential factor, R is the universal gas constant (8.314 J mol⁻¹ K⁻¹), E is the activation energy, (J mol⁻¹), and T is the absolute temperature (K). E_a can be evaluated experimentally from the slope of the plots of $\ln k(T)$ against $(1/T)$ for different temperatures as shown in Eqn. 11.

2.3.2 Adsorption equilibrium isotherms

The relationship for the adsorption process correlates the quantity of the adsorbent (GSAC) used in adsorbing the amount of adsorbate at equilibrium as a function of concentration at constant temperature are called isotherms. For high diluted solutions, the interactions between the molecules of the dissolved adsorbate and the solvent can be neglected, and the process can be modelled based on the assumption of single-gas adsorption [12]. In this case, Langmuir and Freundlich isotherms can be used in describing the equilibrium data. order, pseudo-second-order and intra-particle diffusion were utilized.

The model for the Langmuir Adsorption isotherms

The adsorption isotherms for Langmuir [29] have been employed to describe the adsorption of adsorbate based on the concepts of monolayer on energetically uniform homogeneous solid surfaces. They occur with no interactions among the adsorbate molecules and have the same attraction for the impinging molecules. The expression for Langmuir isotherm can be written in linear form as shown in Eq. 12:

$$\frac{C_e}{q_e} = \frac{1}{K_A q_m} + \frac{1}{q_m} C_e \dots \dots \dots (12)$$

where K_A is the Langmuir constant, which is related to the energy of adsorption (L/mg) and the affinity of the binding sites, and q_m is the maximum adsorption capacity (mg/g). K_A and q_m can be found from the intercept and slope of the plot of C_e/q_e against C_e . Alternatively, Eqn. 12 can be rearranged to give Eqn. 13 as:

$$\frac{1}{q_e} = \frac{1}{q_m} + \frac{1}{K_A q_m C_e} \dots \dots \dots (13)$$

K_A and q_m can be determined from the slope and intercept of the plot of $1/q_e$ versus $1/C_e$ of Eqn. 13.

The model for the Freundlich Adsorption isotherms

In the case of non-ideal adsorption with nonuniform heterogeneous surfaces and occur at sites of different energy levels, the adsorption isotherms for Freundlich [30] have been utilized in describing the process as shown in Eqn. 14:

$$q_e = K_f C_e^{\frac{1}{n}} \dots \dots \dots (14)$$

where K_f and n are the constants of Freundlich isotherms. K_f shows adsorption capacity, while $1/n$ is the adsorption intensity.

Eqn. 15 is the linear form of Eqn. 14 for the Freundlich adsorption isotherms.

$$\ln q_e = \ln K_f + \left(\frac{1}{n}\right) \ln C_e \dots \dots \dots (15)$$

The constants of Freundlich isotherm K_f and n can be obtained from the plot of $\ln q_e$ against $\ln C_e$.

2.3.3 Adsorption thermodynamics

Thermodynamic parameters are essential in understanding the type of the adsorption. These parameters include the changes in the standard enthalpy (ΔH°), standard entropy (ΔS°), and standard Gibbs free energy (ΔG°). Changes in Gibbs free energy can be found at constant temperature and also from Van't Hoff relation as shown in Eqns. 16 and 17, respectively.

$$\Delta G^\circ = \Delta H^\circ - T\Delta S^\circ \dots \dots \dots (16)$$

$$\Delta G^\circ = -RT \ln K_d \dots \dots \dots (17)$$

The changes in the standard entropy and enthalpy, ΔS° and ΔH° can be evaluated from Eqns. 18.

$$\ln K_d = \frac{\Delta S^\circ}{R} - \frac{\Delta H^\circ}{RT} \dots \dots \dots (18)$$

where K_d is the coefficient of distribution which is considered to be equivalent to q_e/C_e .

3. Results and Discussion

3.1 Production and characterization of groundnut shell activated carbon

Activated carbon was produced from the groundnut shells (GSAC) and the products were characterized using various analytical techniques. Field emission dual beam-scanning electron microscopy/focused ion beam (FES-SEM/FIB) was employed for the detailed microstructure of the activated carbon derived from groundnut shells as shown in Figure 2.

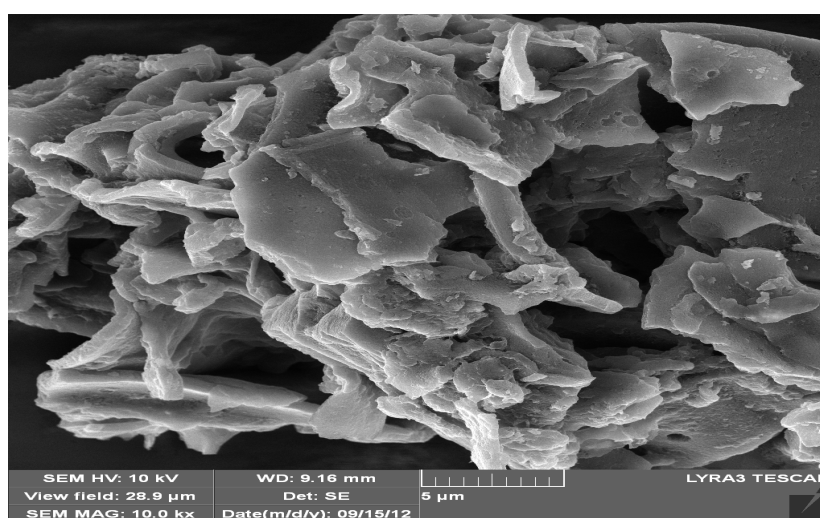


Figure 2. FES-SEM/FIB micrograph of ground nutshell activated carbon (GSAC) produced at 600°C from agricultural byproducts activated with 45% (w/v) of H_3PO_4 .

The Fourier Transform Infrared (FTIR) spectroscope (100 FT-IR, NICOLET) was deployed for the analysis of functional groups of the GSAC products. Different functional groups such as OH and C-H aromatic, C-H aliphatic, C=O and C-O stretching were found in the products.

3.2 Influence of contact time and temperature

The temperature effects and the influence of contact time on the adsorption of DR 1 dye onto the GSAC were concurrently examined at different temperatures and contact time ranging from (301–323 K) and (10–50 min), respectively at pH of 6.23 as shown in Figure 3. It can be observed from the removal efficiency plots that the adsorption of DR 1 dye onto the GSAC increases as the temperature and contact time was raised, sowing the process to be endothermic. The percentage removal of the dye adsorption increased from 29.58 to 59.78% at 301 K, 62.62 to 90.18% at 313 K, and 66.96 to 93.04% at 323 K when the contact time was raised from 10 to 50 minutes, respectively. This perhaps be resulted due to the increase in the kinetic energy of the adsorbate molecules which will lead to an increase in the number of active sites adsorption because of the temperature increase. However, the detailed kinetic analysis is only way that can disclose the actual impacts of process variables and performance of the adsorption at different temperature regimes and contact times.

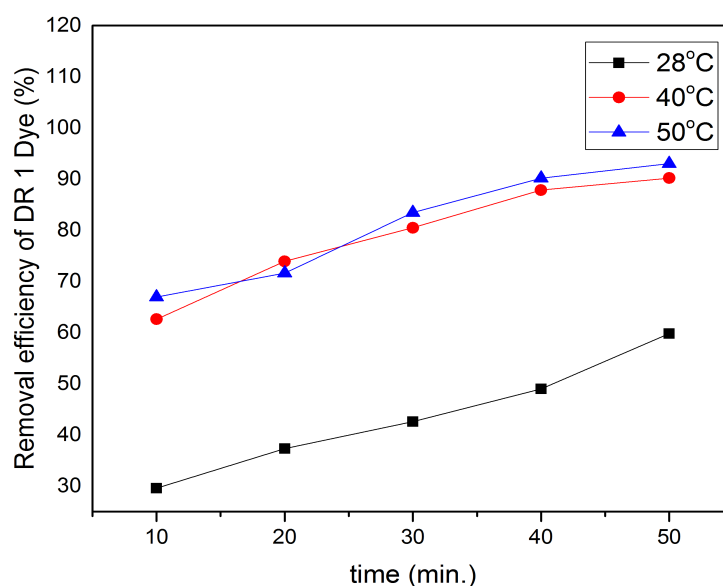


Figure 3. Influences of temperature and contact time on DR 1 dye removal efficiency of GSAC (adsorbent dosage = 1.0 g L^{-1} , dye concentration = 50 mg L^{-1} , and pH of DR 1 dye solution = 6.23).

3.3 Influence of pH and contact time

The effects of contact time and pH on the adsorption of DR 1 dye onto the GSAC were simultaneously investigated at different contact time and solution pH ranging from (10–50 min) and (2.0–10.0) at temperature of 313 K, respectively. The natural pH of the dye solution was adjusted with either 1 molar of HCl or 1 molar of NaOH solutions. One the crucial manipulated variables that influences dye adsorption is the pH of an adsorbate. It controls the magnitude of electrostatic charges which are impacted by the ionized dye molecules. Likewise, studies have been conducted on the isoelectric point (pH_{IEP}) or point of zero charge (pH_{pzc}) in order to understand the mechanism and the rate of dye adsorption using agricultural by-products [31,32]. It can be observed from the plot as shown in Figure 4 that the adsorption of DR 1 dye increases in the acidic medium more predominantly than in the alkaline medium at 313 K. On the other hand, the dye removal efficiency reduced from 73.04 to 66.08, 64.36 to 40.00 and then to 32.92%, at the lowest contact time of 10 minutes when pH was raised from 2 to 3, 4, 8 and 10, respectively. Moreover, the highest adsorbate removal efficiency was determined to be 98.40% at contact time of 50 minutes when pH was only changed to 2.0. Thus, it can be concluded that the adsorption rate of the adsorbate varies with the changes in pH of the working solutions.

3.4 Influence of temperature and initial dye concentration

The influence of temperature and initial dye concentration on the adsorption of DR 1 dye onto the GSAC are exhibited in Figure 5. It was examined at different temperature regimes and initial dye concentrations ranging from (301–323 K) and ($10\text{--}50 \text{ mg L}^{-1}$) at a pH of 2.0 and contact time of 20 minutes, respectively. It can be noted that the removal efficiency of the adsorbate has a linear and inverse relationships with temperature and initial dye concentration, respectively. The removal efficiency was decreased from 88.71 to 72.50% at 301 K, 93.60 to 76.50% at 313 K, and 96.0 to 82.0% at 323 K due to the increase in the initial dye concentration from 10 to 50 mg L^{-1} at contact time of 20 minutes. However, it was increased from 88.71 to 93.6 and then to 96.0% at 10 mg L^{-1} , and from 72.5 to 76.5 and subsequently to 82.0 % when temperature was raised from 301 to 313, and then to 323 K, respectively.

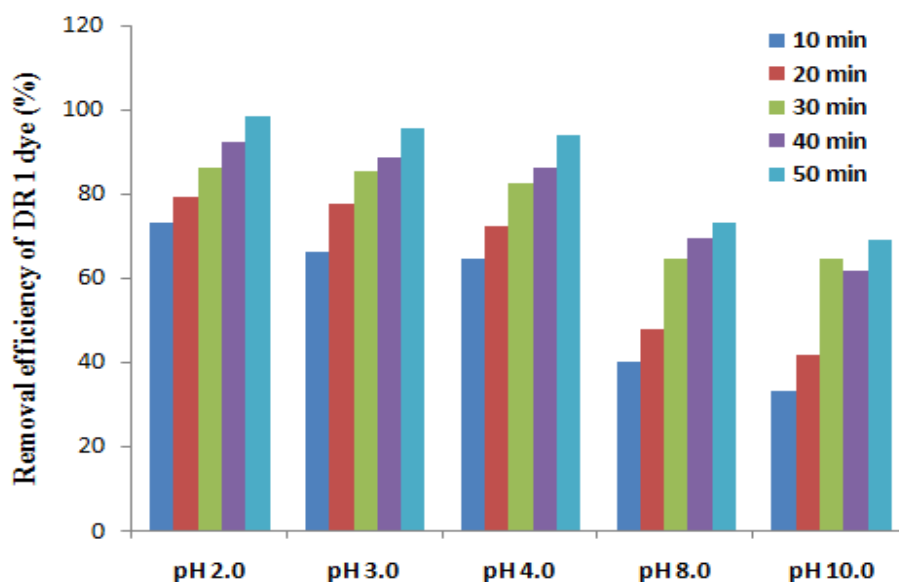


Figure 4. Influences of contact time and solution pH on DR 1 dye removal efficiency of GSAC (adsorbent dosage = 1.0 g L^{-1} , dye concentration of 50 mg L^{-1} , and temperature of 313 K).

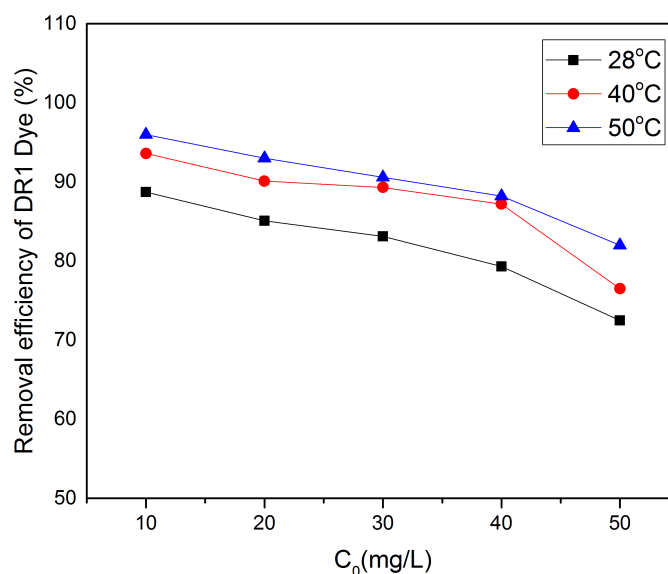


Figure 5. Influences of initial dye concentration and temperature on DR 1 dye removal efficiency of GSAC (adsorbent dosage of 1.0 g L^{-1} , dye solution pH of 2.0, contact time of 20 minutes).

3.5 Analysis for adsorption kinetics

The results found from the model fittings of DR 1 dye adsorption onto the GSAC with pseudo first-order, pseudo second-order kinetic expressions, and intra-particle diffusion using Weber and Morris [33] at 28°C , 60°C and 80°C are shown in Figures 6, 7 and 8, respectively. From the plots of adsorption kinetics, it can be observed that both pseudo first-order kinetics and pseudo second-order rate expression for the DR 1 dye adsorption onto the GSAC have a good agreement with the experimental data as exhibited in Figures 6 and 7. However, it can be noted that the linear fittings of t/q_t versus t plots show a better agreement of the kinetic data with the model of pseudo second-order kinetic expression at different temperatures. This remarkable difference can be seen from the results presented in Table 1 for the models' comparisons.

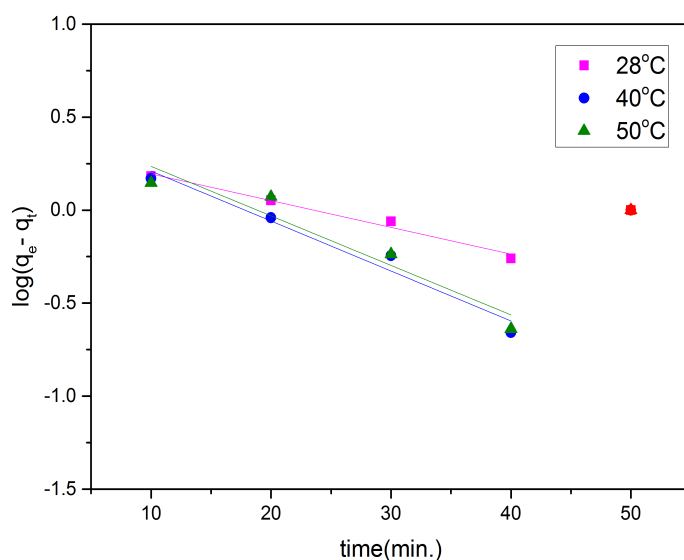


Figure 6. Pseudo-first-order kinetics for adsorption of DR 1 dye onto the GSAC at 50 mg/L initial dye concentration, dye solution pH of 2.0 and different temperature regimes.

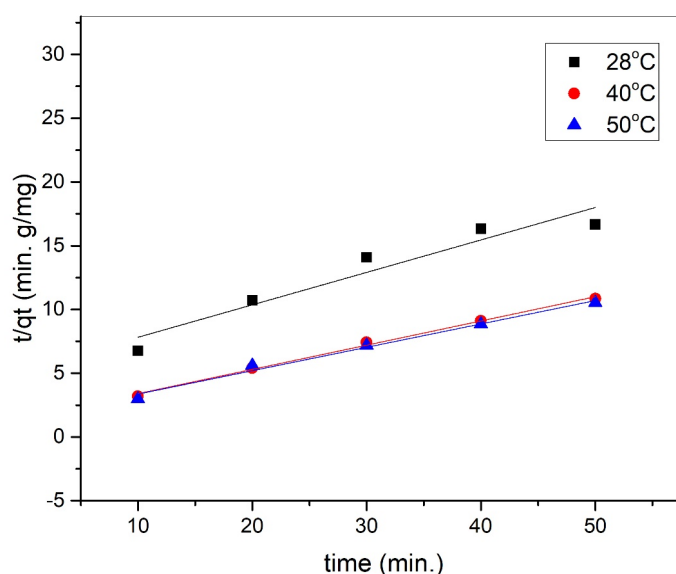


Figure 7. Pseudo-second-order kinetics for adsorption of DR 1 dye onto the GSAC at 50 mg/L initial dye concentration, dye solution pH of 2.0 and different temperature regimes.

Table 1. Comparison of the pseudo-first-order and pseudo-second-order kinetics models for the DR 1 dye adsorption onto the GSAC at different temperatures and pH of 2.0

Temp. (K)	q_e, exp (mg g^{-1})	Pseudo-first-order kinetic model				Pseudo-second-order kinetic model				
		q_e, cal (mg g^{-1})	k_{obs} (min^{-1})	Pearson's r	Adj. R^2	q_e, cal (mg g^{-1})	k_{obs} ($\text{g mg}^{-1}\text{min}^{-1}$)	r_{AO} ($\text{mg L}^{-1}\text{min}^{-1}$)	Pearson's r	Adj. R^2
301	3.00	2.179	3.31×10^{-2}	-0.992	0.975	3.929	4.82×10^{-2}	7.44×10^{-1}	0.963	0.902
313	4.61	3.010	6.19×10^{-2}	-0.983	0.949	5.263	12.67×10^{-2}	35.10×10^{-1}	0.998	0.995
323	4.75	3.171	6.13×10^{-2}	-0.963	0.891	5.464	11.96×10^{-2}	35.71×10^{-1}	0.995	0.986

Table 2. Comparison of the pseudo-first-order and pseudo-second-order kinetics models for the DR1 dye adsorption onto the GSAC at different pH and temperature of 40°C.

pH	Pseudo-first-order kinetic model					Pseudo-second-order kinetic model				
	q_e, exp (mg g^{-1})	q_e, cal (mg g^{-1})	k_{obs} (min^{-1})	Pearson's s r	Adj. R^2	q_e, cal (mg g^{-1})	k_{obs} ($\text{g mg}^{-1}\text{min}^{-1}$)	r_{A0} ($\text{mg L}^{-1}\text{min}^{-1}$)	Pearson's s r	Adj. R^2
2.0	3.992	2.282	5.12×10^{-2}	-0.979	0.946	5.353	3.08×10^{-2}	0.88	0.997	0.992
3.0	3.857	2.386	4.89×10^{-2}	-0.998	0.994	5.342	2.64×10^{-2}	0.75	0.998	0.995
4.0	3.837	2.474	4.65×10^{-2}	-0.991	0.973	5.317	2.32×10^{-2}	0.66	0.996	0.989
8.0	3.863	4.492	7.89×10^{-2}	-0.976	0.929	4.873	1.23×10^{-2}	0.29	0.988	0.968
10.0	4.104	3.328	5.97×10^{-2}	-0.858	0.604	4.975	9.27×10^{-3}	0.23	0.963	0.904

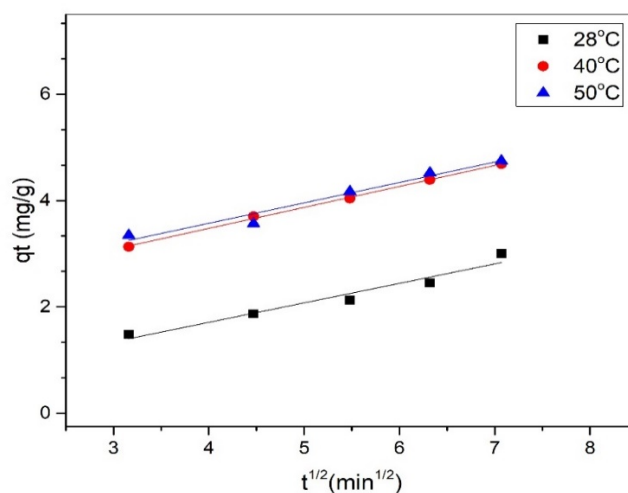


Figure 8. Intra-particle diffusion kinetics for adsorption of DR 1 dye onto the GSAC at 50 mg/L initial dye concentration, dye solution pH of 2.0 and different temperature regimes.

Table 3. Webber-Morris intra-particle diffusion model for the kinetics of DR1 dye adsorption onto the GSAC at different temperatures and pH of 2.0.

Temp. (K)	k_{id} ($\text{mg min}^{-1/2}\text{g}$)	$C_{\text{id, cal}}$ (mg g^{-1})	Pearson's r	Adj. R^2
301	0.37 ± 0.05	0.24 ± 0.25	0.977	0.940
313	0.39 ± 0.01	1.90 ± 0.05	0.999	0.998
323	0.38 ± 0.04	2.04 ± 0.22	0.983	0.956

Table 4. Webber-Morris intra-particle diffusion model for the kinetics of DR1 dye adsorption onto the GSAC at different pH and temperature of 40°C.

pH	k_{id} ($\text{mg min}^{-1/2}\text{g}$)	$C_{\text{id, cal}}$ (mg g^{-1})	Pearson's r	Adj. R^2
2.0	0.317 ± 0.02	2.601 ± 0.09	0.996	0.990
3.0	0.366 ± 0.02	2.185 ± 0.12	0.995	0.986
4.0	0.377 ± 0.02	1.996 ± 0.14	0.994	0.983
8.0	0.457 ± 0.05	0.528 ± 0.30	0.979	0.945
10.0	0.482 ± 0.07	0.165 ± 0.51	0.949	0.867

The values obtained for the Pearson's r and adjusted R^2 for the pseudo second-order model are slightly higher than that of pseudo first-order model at all temperature regimes. Similarly, the observed kinetics at 40°C for different pH values of the working solutions showed a better agreement with the model of pseudo second-order kinetics than pseudo first-order rate law. The summaries of the results are compared in Tables 1 and 2.

The possibility for intra-particle diffusion step to control the adsorption rate of DR 1 dye onto the GSAC was analysed with the aid of Webber and Morris model. The results for the adsorption of DR 1 dye at different temperature regimes are depicted in Figure 8. The Pearson's r and adjusted R^2 are exhibited in Table 3. Likewise, the observed kinetic data generated at 40°C for different pH values of the working solutions were fitted with the kinetic model for intra-particle diffusion. The results obtained are shown in Table 4 for comparison with that of Table 2. After careful observations from the results, the kinetic model for the pseudo second-order appears to be the best model that describe the kinetics at 301, 313, and 323 K, and solution pH of 2.0, 3.0, 4.0, 8.0, and 10.0. The activation energy (E_a) was evaluated as 6.35 kJ/mol. It was noted that the observed specific adsorption rate constant (k_{obs}) which characterize the adsorption kinetics for the pseudo second-order decreased by 1.09 and 1.19 folds when the temperature was raised from 301 K to 313 K, and to 323 K, respectively. Hence, it can be inferred that the k_{obs} has an inverse relationship with temperature.

3.6 Analysis for adsorption equilibrium isotherms

The equilibrium relationship for the adsorption are pertinent in the design and development of adsorbents as well as adsorption processes. This relationship is used to describe how adsorbent active sites interact with adsorbate molecules in adsorption. Langmuir and Freundlich adsorption isotherms were utilized for fitting the equilibrium data for the adsorption of DR 1 dye onto the GSAC. Table 5 presents the results of the model parameters for the adsorption isotherms with their correlation coefficients, coefficient of determination, Pearson's r , and adjusted R^2 .

Table 5. Langmuir and Freundlich isotherm constants for the adsorption of DR1 dye onto the GSAC at various temperatures and pH of 2.0.

Temp. (K)	Langmuir isotherm model		Freundlich isotherm model					
	q_{max} (mg g ⁻¹)	K_A (L mg ⁻¹)	Pearson's r	Adj. R^2	K_F (mg ^{1-1/n} L ^{1/n} g ⁻¹)	n	Pearson's r	Adj. R^2
301	5.105±0.057	0.184±0.04	0.999	0.997	0.886	1.72	0.989	0.970
313	4.414±0.010	0.565±0.06	0.997	0.992	1.315	2.01	0.969	0.919
323	5.083±0.009	0.493±0.04	0.997	0.992	1.524	2.04	0.990	0.974

These results show a good agreement between the experimental data and the two tested models for the adsorption. It can be noted that the equilibrium data for the three (3) different process conditions are well fitted. For Langmuir adsorption isotherms, it can be inferred that there is uniform homogeneity of each molecule of the DR 1 dye adsorbed on the active site of the GSAC surfaces. This is due to the concept of monolayer adsorption of the adsorbate molecules on the outer surfaces of the GSAC with the same attraction, no interactions, and equal activation energy among them. However, in the case of the Freundlich adsorption isotherms, the equilibrium interactions are characterized by the non-ideality, non-uniformity and heterogeneity of the adsorbate molecules adsorption on the active sites of the GSAC surfaces. It can be observed that the exponents, n obtained from the analysis of Freundlich adsorption

isotherms are greater than 1 as shown in Table 5. Based on these values, the adsorption is considered to be favourable.

3.7 Analysis of thermodynamics parameters

Thermodynamic analysis was carried out in order to determine the thermodynamic parameters such the changes in the standard Gibb's free energy (ΔG°), enthalpy (ΔH°), and entropy (ΔS°) for the adsorption process. The results are presented in Table 6. The negative value of ΔG° indicates the feasibility of the adsorption process to be spontaneous. The positive values of ΔH° and ΔS° confirm that the adsorption process is endothermic and there is an increasing randomness at the interface of solid-liquid during the adsorption of the DR 1 dye onto the GSAC.

Table 6. Thermodynamic parameters of DR 1 dye adsorption onto the GSAC.

Temperature(K)	Parameters		
	ΔG° (kJ/mol)	ΔH° (kJ/mol)	ΔS° (kJ/mol K)
301	-2.99	18.31	0.07
313	-3.50		
323	-4.42		

4. Conclusions

Kinetics, equilibrium, and thermodynamic studies for the adsorption of DR 1 dye onto the GSAC were successfully conducted. The findings of this investigation indicate that activated carbon derived from groundnut shell agricultural by products can be successfully employed for the adsorption of DR 1 dye. The results depicted that the pseudo second order kinetic was best model that described the adsorption of DR 1 dye with the values of correlation coefficient of 0.993, 0.998, 0.995, and coefficient of determination of 0.979, 0.995 and 0.986 at 28°C, 40°C, and 50°C respectively. It was noted that the k_{obs} above the temperature regime of 313 K has an inverse relationship with temperature. It was found that k_{obs} for its kinetics increased by 61.96% and 59.70% when the temperature was increased from 301 K to 313 K, and from 301 K to 323 K, respectively. These results disclose that adsorption will not favourable above the temperature regime of 313K. The E_a was determined as 6.35 kJ/mol. Based on the models for the equilibrium adsorption isotherms, Langmuir isotherm was the best model to fit the equilibrium data for the DR 1 dye adsorption. Thermodynamic analysis reveals the process was spontaneous since the ΔG is negative, while the ΔH and ΔS were found to be 19.46 kJ/mol and 0.072 kJ/mol K, respectively.

Acknowledgments One of the authors Umar Isah Abubakar, PhD thanks Allah SWT for everything. The authors gratefully acknowledge the supports of Engr. Adamu S, Department of Chemical Engineering, King Fahd University of Petroleum and Minerals (KFUPM), Dr Yamani ZH, and Dr Hakeem AS, Centre of Excellence in Nanotechnology (CENT), Research Institute, KFUPM, Saudi Arabia for the analysis of activated carbon using FES-SEM/FIB.

Disclosure statements

Conflict of Interest: The authors declare that there are no conflicts of interest.

Compliance with Ethical Standards: This research article does not contain any studies involving human or animal subjects.

References

- [1] P. Kumar, R. Agnihotri, K. L. Wasewar, H. Uslu, C. K. Yoo, Status of adsorptive removal of dye from textile industry effluent. *Des. Water Treat.* 50 (2012) 226–244.
- [2] K. Rasool, S. H. Woo, D. S. Lee, Simultaneous removal of COD and Direct Red 80 in a mixed anaerobic sulfate-reducing bacteria culture. *Chem. Eng. J.* 223 (2013) 611-616.
- [3] S. Wijetunga, L. Xiufen, R4T. Wenquan, J. Chen, Evaluation of the efficacy of up flow anaerobic sludge blanket reactor in removal of color and reduction of COD in real textile wastewater. *Biores. Technol.* 99 (2008) 3692-3699.
- [4] W. H. Cheung, Y. Z. Szeto, G. McKay, Enhancing the adsorption capacities of acid dyes by chitosan nanoparticles. *Biores. Technol.* 100 (2009)1143-1148.
- [5] T. L. Hu, S. C. Wu, Assessment of the effect of azo dye RP2B on the growth of a nitrogen fixing cyanobacterium – *Anabaena* sp. *Biores. Technol.* 77 (2001) 93-95.
- [6] K. Mazeau, M. Wyszomirski, Modeling of Congo red adsorption on the hydrophobic surface of cellulose using molecular dynamics. *Cellulose* 19(5) (2012) 1495-1506.
- [7] M. Skowronek, B. Stopa, L. Konieczny, J. Rybarska, B. Piekarska, E. Szneler, G. Bakalarski, I. Roterman, Self-assembly of Congo Red—A theoretical and experimental approach to identify its supramolecular organization in water and salt solutions. *Biopolymers.* 46(5) (2012) 267-281.
- [8] A. K. Kondru, P. Kumar, S. Chand, Catalytic wet peroxide oxidation of azo dye (Congo red) using modified Y zeolite as catalyst. *J. Haz. Mats.* 166 (2009) 342–347.
- [9] F. A. Pavan, S. L. P. Dias, E. C. Lima, E. V. Benvenuti, Removal of congo red from aqueous solution by anilinepropylsilica xerogel, *Dyes Pigm.* 76 (2009) 64–69.
- [10] N. P. Raval, P. U. Shah, N. K. Shah, Adsorptive amputation of hazardous azo dye Congo red from wastewater: a critical review. *Environ. Sci. Pollut. Res.* 23(15) (2016) 14810–14853.
- [11] Z. J. Yang, J. J. Wei, H. X. Yang, L. Liu, H. Liang, Y. Z. Yang, Mesoporous CeO₂ hollow spheres prepared by Ostwald ripening and their environmental applications. *Euro. J. Inorg. Chemist.* 21 (2016) 3354-3359.
- [12] A. Dąbrowski, Adsorption — from theory to practice. *Adv. in Colloid and Inter. Sci.* 93 (2001) 135-224.
- [13] T. Robinson, G. McMullan, R. Marchant, P. Nigam Remediation of dyes in textile effluent: a critical review on current treatment technologies with a propose alternative. *Biores. Technol.* 77 (2001) 247-255.
- [14] P. V. Prasad, V. G. Kakani, H. D. Upadhyaya (2010) Growth and production of groundnut in UNESCO Encyclopedia. 1-26.
- [15] B. H. Hameed, A. A. Ahmad, N. Aziz, Isotherms, kinetics and thermodynamics of acid dye adsorption on activated palm ash. *Chem. Eng. J.* 133 (2007) 195-203.
- [16] M. Belhachemi, F. Addoun, Adsorption of congo red onto activated carbons having different surface properties: Studies of kinetics and adsorption equilibrium. *Desalin. Water Treat.* 37 (2012) 122-129.
- [17] A. Ebrahimi, E. Pajootan, M. Arami, M. Bahrami, Optimization, kinetics, equilibrium, and thermodynamic investigation of cationic dye adsorption on the fish bone. *Desalin. Water Treat.* 53 (2013) 1-11.
- [18] M. A. Ahmad, M. A. Puad, and O. S. Bello, Kinetic, equilibrium and thermodynamic studies of synthetic dye removal using pomegranate peel activated carbon prepared by microwave-induced KOH activation. *Water Resources and industry,* 6 (2014) 18-35.

- [19] U. A. Isah, G. Abdulraheem, S. Bala, S. Muhammad, M. Abdullahi (2015) Kinetics, equilibrium and thermodynamics studies of C.I. Reactive Blue 19 dye adsorption on coconut shell based activated carbon. *International. Biodetrio. & Biodegrada.* J. 102:265-273.
- [20] K. Rasool, D. S. Lee (2015) Characteristics, kinetics and thermodynamics of Congo Red biosorption by activated sulfidogenic sludge from an aqueous solution. *Int. J. Environ. Sci. Technol.* 12(2):571-580.
- [21] A. H. Jawad, R. A. Rashid, M. A. M. Ishak, L. D.L. D. Wilson, (2016). Adsorption of methylene blue onto activated carbon developed from biomass waste by H₂SO₄ activation: kinetic, equilibrium and thermodynamic studies. *Desalination and Water Treatment*, 57(52), 25194-25206.
- [22] M. Zubair, N. Jarrah, M. S. Manzar, M. Al-Harhi, M. Daud, N. D. Mu'azu, N. D. Haladu, (2017). Adsorption of eriochrome black T from aqueous phase on MgAl-, CoAl- and NiFe-calcined layered double hydroxides: kinetic, equilibrium and thermodynamic studies. *Journal of molecular liquids*, 230, 344-352
- [23] G. Torğut, K. Demirelli, (2018). Comparative adsorption of different dyes from aqueous solutions onto polymer prepared by ROP: kinetic, equilibrium and thermodynamic studies. *Arabian Journal for Science and Engineering*, 43(7) 3503-3514.
- [24] M. Sarabadan, H. Bashiri, S. M. Mousavi, (2019). Removal of crystal violet dye by an efficient and low-cost adsorbent: Modeling, kinetic, equilibrium and thermodynamic studies. *Korean Journal of Chemical Engineering*, 36(10),1575-1586.
- [25] D. Lin, F. Wu, Y. Hu, T. Zhang, C. Liu, Q. Hu, T. HKo, (2020). Adsorption of dye by waste black tea powder: parameters, kinetic, equilibrium, and thermodynamic studies. *Journal of Chemistry*, 2020.
- [26] S. Lagergren (1898) Zur theorie der sogenannten adsorption gelöster stoffe. *Kungliga Svenska Vetenskapsakademiens. Handlingar, Band*, 24:1-39.
- [27] Y-S. Ho G. McKay (1999) Pseudo-second order model for sorption processes. *Process Biochem.* 34:451-465.
- [28] W. Weber, J. Morris (1963) Kinetics of adsorption on carbon from solution. *J. Sanit Eng. Div. Am. Soc. Civ. Eng.* 89:31-60.
- [29] S. Arrhenius (1916) Über die Reaktionsgeschwindigkeit bei der Inversion von Rohrzucker durch Säuren *Zeitschrift für physikalische Chemie.* 4:226-248
- [30] I. Langmuir (1916) The constitution and fundamental properties of solids and liquids. *Part I Solids Journal of American Chem. Soc.* 38:2221-2295.
- [31] H. Freundlich (1907) Ueber Kolloidfällung und Adsorption. *Zeitschrift für Chemie und Industrie der Kolloide.* 1:321-331.
- [32] Y. Önal, C. Akmil-Başar, D. Eren, C. Sarıcı-Özdemir, T. Depci (2006) Adsorption kinetics of malachite green onto activated carbon prepared from Tuncbilek lignite. *Journal of hazardous materials*, 128:150-157.
- [33] A. Poghossian (1997) Determination of the p*H*_{pzc} of insulators surface from capacitance–voltage characteristics of MIS and EIS structures. *Sensors and Actuators B Chemical*, 44:551-553.

(2022) ; <http://www.jmaterenvirosci.com>